Nitric Oxide as an Electron Donor, an Atom Donor, an Atom Acceptor, and a Ligand in Reactions with Atomic Transition-Metal and Main-Group Cations in the Gas Phase

ARTICLE *in* THE JOURNAL OF PHYSICAL CHEMISTRY A · JANUARY 2006

Impact Factor: 2.69 · DOI: 10.1021/jp0553939 · Source: PubMed

5 AUTHORS, INCLUDING:

Voislav Blagojevic
Vida Holdings Corp.
42 PUBLICATIONS **707** CITATIONS
SEE PROFILE

Michael Jarvis
AB SCIEX
24 PUBLICATIONS **223** CITATIONS
SEE PROFILE

Gregory K Koyanagi
York University
58 PUBLICATIONS **1,227** CITATIONS
SEE PROFILE

Diethard K Bohme
York University
422 PUBLICATIONS **8,852** CITATIONS
SEE PROFILE

Nitric Oxide as an Electron Donor, an Atom Donor, an Atom Acceptor, and a Ligand in Reactions with Atomic Transition-Metal and Main-Group Cations in the Gas Phase

Voislav Blagojevic, Eric Flaim, Michael J. Y. Jarvis, Gregory K. Koyanagi, and Diethard K. Bohme*

Department of Chemistry, Centre for Research in Mass Spectrometry and Centre for Research in Earth and Space Science, York University, Toronto, Ontario, Canada M3J 1P3

Received: September 22, 2005

The room-temperature reactions of nitric oxide with 46 atomic cations have been surveyed systematically across and down the periodic table using an inductively-coupled plasma/selected-ion flow tube (ICP/SIFT) tandem mass spectrometer. Rate coefficients and product distributions were measured for the reactions of first-row cations from K^+ to Se^+, of second-row cations from Rb^+ to Te^+ (excluding Tc^+), and of third-row cations from Cs^+ to Bi^+. Reactions both first and second order in NO were identified. The observed bimolecular reactions were thermodynamically controlled. Efficient exothermic electron transfer was observed with Zn^+, As^+, Se^+, Au^+, and Hg^+. Bimolecular O-atom transfer was observed with Sc^+, Ti^+, Y^+, Zr^+, Nb^+, La^+, Hf^+, Ta^+, and W^+. Of the remaining 32 atomic ions, all but 8 react in novel termolecular reactions second order in NO to produce NO^+ and the metal−nitrosyl molecule, the metal−monoxide cation and nitrous oxide, and/or the metal−nitrosyl cation. K^+, Rb^+, Cs^+, Ga^+, In^+, Tl^+, Pb^+, and Bi^+ are totally unreactive. Further reactions with NO produce the dioxide cations CaO_2^+, TiO_2^+, VO_2^+, CrO_2^+, SrO_2^+, ZrO_2^+, NbO_2^+, RuO_2^+, BaO_2^+, HfO_2^+, TaO_2^+, WO_2^+, ReO_2^+, and OsO_2^+ and the still higher order oxides WO_3^+, ReO_3^+, and ReO_4^+. NO ligation was observed in the formation of $CaO^+(NO)$, $ScO^+(NO)$, $TiO^+(NO)$, $VO^+(NO)_{1-3}$, $VO_2^+(NO)_{1-3}$, $SrO^+(NO)$, $SrO_2^+(NO)_{1,2}$, $RuO^+(NO)_{1-3}$, $RuO_2^+(NO)_{1,2}$, $OsO^+(NO)_{1-3}$, and $IrO^+(NO)$. The reported reactivities for bare atomic ions provide a benchmark for reactivities of ligated atomic ions and point to possible second-order NO chemistry in biometallic and metal-surface environments leading to the conversion of NO to N_2O and the production of metal−nitrosyl molecules.

Introduction

Gaseous nitric oxide has a long and extensive history of relevance in atmospheric and ionospheric chemistry and as a pollutant in combustion. But more recently, because of its biochemical activity, nitric oxide has burst upon the scene of neuroscience, particularly neurotransmission and neurobiology, as well as cardiovascular physiology, immunology, and carcinogenesis.[1−4] "This new role has reinvigorated research into the fundamental chemistry of this simple molecule, much to the delight of chemists, and led *Science* magazine to designate NO Molecule of the Year in 1992".[4] It also prompted *Chemical & Engineering News* to assign "superstar" status to this molecule a year later.[2]

Metal atoms and ions are often implicated in the chemical and biochemical activity of NO. For example, the interaction of transition metals such as Ti, Pb, Zn, Fe, V, Mn, and Ni with NO may be involved in the photodissociative production of smog in highly polluted environments.[5] Reactions of NO on metal surfaces and zeolites doped with metals are important in the development of efficient catalysts for use in catalytic converters or for industrial applications of NO decomposition.[6,7] Gas-phase chemical cycles mediated by transition-metal cations and their oxides have been identified for the catalytic conversion of N_2O and CO to N_2 and CO_2.[8,9] The binding of NO to metalloenzymes and metalloporphorins has been implicated in the important biological functions of NO.[10]

Much of the chemical and biochemical activity of NO is due to the unique free radical nature of this diatomic molecule along with the relative ease of removing its unpaired electron (IE(NO) = 9.264 eV).[11] In this study we survey the kinetic ability of NO to transfer an electron or donate an oxygen atom to isolated atomic cations. We have accomplished this with 46 atomic cations including transition-metal and main-group cations. Previous measurements with atomic ions have demonstrated rapid electron transfer, $k > 10^{-10}$ cm^3 molecule^{-1} s^{-1}, from NO to H^+, He^+, C^+, N^+, F^+, Ne^+ (dissociative electron transfer), S^+, Cl^+, and Ar^+ but not to Na^+, K^+, Kr^+, O^+, and Si^+, $k < 10^{-10}$ cm^3 molecule^{-1} s^{-1}.[12] Of particular note is the observation of N-atom transfer, reaction 1b, proceeding in competition with electron transfer, reaction 1a, with $X^+ = N^+$ (15%)[13] and F^+ (10%).[14]

$$X^+ + NO \rightarrow NO^+ + X \quad (1a)$$

$$\rightarrow XN^+ + O \quad (1b)$$

Apparently, the first measurement of a reaction of a transition-metal cation with NO in the gas phase was that with Ti^+ reported in 1974 by Biondi et al.[15] Ti^+ ions were produced with a titanium−tungsten filament. Rate coefficients for reactions with NO were measured for both Ti^+ and Th^+ in a drift-tube mass spectrometer over an energy range from thermal energies (300 K) to 2 eV (mean kinetic energy). In 1985, the drift tube was coupled to a zirconium-ion discharge containing $ZrBr_4$ to measure the rate coefficient for the reaction of Zr^+ with NO

* Corresponding author. E-mail dkbohme@yorku.ca. Phone: 416-736-2100, ext 66188. Fax 416-736-5936.

10.1021/jp0553939 CCC: $30.25
Published on Web 11/17/2005

over a similar energy range.[16] In 1981 ion cyclotron resonance (ICR) mass spectroscopy, in which metal cations were produced by laser volatilization/ionization, provided results for go/no go experiments that indicated fast oxidation reactions of NO with Ti^+, Zr^+, and Nb^+ and nonoxidation with V^+.[17] Somewhat surprisingly, there appear not to have been any other previous measurements of atomic metal and main-group cation reactions with NO. In the experiments reported here the atomic cations are generated in an inductively-coupled plasma (ICP) of argon at ca. 5500 K. The ions are then injected into a flow tube to measure their reactivities with NO. This combined ICP/SIFT technique[18,19] was used to examine the reactivities of 46 atomic cations including 29 transition-metal and 17 main-group cations, most of which have not previously been investigated by others. The experiments were performed over a high range of NO additions, and this led to the discovery of unexpected second-order NO chemistry that has previously also not been reported. These latter results may have important implications for NO^+, MO^+, N_2O, and nitrosyl formation in environments containing charged metals and elevated levels of nitric oxide gas. Certainly the results reported here for the interaction of bare atomic metal ions with NO will serve as a valuable benchmark for similar interactions in the condensed phase involving ligated metal ions.

Experimental Method

The experimental results reported here were obtained using the selected-ion flow tube (SIFT) tandem mass spectrometer in the Ion-Chemistry Laboratory at York University, described in detail elsewhere.[19] Recently, it has been modified to accept ions generated in an inductively coupled plasma (ICP) torch through an atmosphere/vacuum interface (ELAN series, Perkin-Elmer SCIEX). The ICP ion source and interface have also been described previously.[18] Solutions containing the metal salt of interest having concentration of ca. 5 μg L^{-1} were peristaltically pumped via a nebulizer into the plasma. The nebulizer flow was adjusted to maximize the ion signal detected downstream of the SIFT. The sample solutions were prepared using atomic spectroscopy standard solutions commercially available from SPEX, Teknolab, J. T. Baker Chemical Co., Fisher Scientific Co., Perkin-Elmer, and Alfa Products. A single-isotope solution was used for Ca^+ (m/z 44) from readily soluble $CaCO_3$ (>98.5% isotope purity, Oak Ridge National Laboratory (Isotope Business Office)) to avoid overlap with Ar^+ (m/z 40) in the ICP ion selection. Aliquots of standard solutions were diluted with highly purified water produced in the Millipore Milli-Qplus ultrapure water system. The final concentrations were varied within 5−20 ppm interval to achieve suitable intensity of the resultant ion beam. Normally, a stabilizing agent was added to each solution to prevent precipitation. That was either HNO_3 or HCl for acid-stabilized salts or KOH for those base-stabilized.

Atomic ions emerge from the ICP at a nominal ion temperature of 5500 K with corresponding Boltzmann state distributions. These distributions have been derived from available optical spectra[20,21] and reported by us previously.[22] The calculations show that excited states of the main-group elemental cations except Ba^+ are high in energy and contribute little (never more than 10%) to the total ion population at 5500 K. The ground ^2S state of Ba^+ contributes 44% and the excited ^2D state 55% at 5500 K. The state distributions are more variable for the transition-metal cations. Excited states contribute 20% or less toward the populations of Cr^+, Mn^+, Ni^+, Cu^+, Zn^+, Rh^+, Pd^+, Ag^+, Cd^+ Re^+, Au^+, and Hg^+ and 50% or more toward the populations of Ti^+, Y^+, Zr^+, Nb^+, La^+, and Ir^+ with Sc^+, V^+, Fe^+, Co^+, Mo^+, Ru^+, Hf^+, Ta^+, W^+, and Pt^+ having intermediate distributions.

After extraction from the ICP, the plasma ions may experience both radiative electronic-state relaxation and collisional electronic-state relaxation. The latter may occur with argon as the extracted plasma cools upon sampling and then by collisions with He atoms in the flow tube (ca. 4×10^5 collisions) prior to the reaction region, but the actual extent of electronic relaxation (either radiative or collisional) is not known and is difficult to assess. Almost all of the electronic states of the transition-metal ions have positive parity; electric dipole transitions between states of the same parity are forbidden (Laporte rule).[23a] This means that radiative transitions between different states in metal cations can be achieved only by either magnetic dipole or electric quadrupole radiation. The probabilities for these transitions are very low,[23b] and the resulting radiative lifetimes are of the order of seconds or larger. The time interval in the ICP/SIFT experiments between the exit of the ICP source and the entrance in the reaction region is ~20 ms, and therefore no major modification of state distributions can occur in this time interval by forbidden radiative decay. That having been said, there were no indications of excited-state effects in our previous measurements of reactions of atomic cations derived from the same ICP source with N_2O, except with Pt^+.[22] The many collisions experienced by the atomic cations with the quite polarizable Ar atoms as they emerge from the ICP and the ca. 10^4 collisions with He atoms in the flow tube (the helium buffer gas pressure was 0.35 ± 0.01 Torr) appear to be sufficient to provide for the thermalization of the excited states and ensure that the atomic ions reach a translational temperature equal to the tube temperature of 295 ± 2 K prior to entering the reaction region. However, the exact extent of electronic relaxation is uncertain. Clues to the presence of excited electronic states of the atomic ions in the reaction region can be found in the products observed and the shape (linearity) of the semilogarithmic decay of the reacting atomic ion upon addition of neutral reactant. All such indications, often including the observation of linearity for more than one decade of signal decay, are that the exited states are relaxed or that they react with the same rate and give the same product as the ground-state species. The semilogarithmic decay for most of the reactive cations investigated was observed to be linear for more than one decade. A decay of much more than the percentage of excited states calculated to be present within the ICP indicates cannot be attributed solely to excited states.

The NO reagent gas had a nominal purity of 99.5% (BOC Gases) within the gas tank. In situ chemical ionization experiments with atomic metal cations derived from the ICP source provided further insight into the levels of impurities *within the reaction region*. In separate experiments we have found that some metal oxide ions (ScO^+, ZrO^+, LaO^+) react with NO_2 to produce NO^+ but do not form NO^+ with NO. Therefore the failure to observe downstream NO^+ with these metal oxide ions with added NO can provide an upper limit to the level of NO_2 impurity in the NO. Such experiments have provided a conservative upper limit of 0.5%. An analogous approach was used to arrive at an upper limit of 1% to the level of N_2O impurity in NO. In this case CeN^+ was used as the indicator because our experiments established that Ce^+ reacts with N_2O to produce CeN^+ with $k = 1.3 \times 10^{-10}$ cm^3 $molecule^{-1}$ s^{-1}.[22] No CeN^+ was observed when NO was added to Ce^+. Also, failure to observe AsO^+ with added NO indicated levels for possible N_2O impurities, of less than 0.1% in the reaction region because we have shown that As^+ reacts with N_2O to produce AsO^+ ($k = 2.7 \times 10^{-10}$ cm^3 $molecule^{-1}$ s^{-1})[22] and it is known now that subsequent electron transfer of NO to AsO^+ is

TABLE 1: Rate Coefficients (cm^3 $molecule^{-1}$ s^{-1}), Reaction Efficiencies (k/k_c), and Higher Order Product Ions Measured for Reactions of First-Row Metal Cations with Nitric Oxide in Helium at 0.35 ± 0.01 Torr and 295 ± 2 K

reaction[a]	k[b]	k_c[c]	k/k_c	higher order product ions
$K^+ + NO \rightarrow NR$	$\leq 1 \times 10^{-12}$	7.8×10^{-10}	$\leq 10^{-3}$	
$Ca^+ + NO + NO \rightarrow CaO^+ + N_2O$	7.0×10^{-12}	7.6×10^{-10}	9.2×10^{-3}	CaO_2^+,$CaO^+(NO)$
$Sc^+ + NO \rightarrow ScO^+ + N$	3.3×10^{-11}	7.6×10^{-10}	0.043	$ScO^+(NO)$
$Ti^+ + NO \rightarrow TiO^+ + N$	1.2×10^{-10}	7.5×10^{-10}	0.16	TiO_2^+, $TiO^+(NO)$, NO^+
$V^+ + NO + NO \rightarrow VO^+ + N_2O$	2.1×10^{-11}	7.4×10^{-10}	0.028	VO_2+, NO^+, $VO^+(NO)_{1-3}$, $VO_2^+(NO)_{1-3}$
$Cr^+ + NO + NO \rightarrow CrO^+ + N_2O$ (0.8) $\rightarrow NO^+ + CrNO$ (0.2)	9.2×10^{-12}	7.4×10^{-10}	0.012	CrO_2^+
$Mn^+ + NO + NO \rightarrow NO^+ + MnNO$ (0.7) $\rightarrow MnO^+ + N_2O$ (0.3)	3.3×10^{-12}	7.3×10^{-10}	0.005	
$Fe^+ + NO + NO \rightarrow FeO^+ + N_2O$	1.8×10^{-11}	7.3×10^{-10}	0.025	NO^+
$Co^+ + NO + NO \rightarrow CoO^+ + N_2O$	4.2×10^{-11}	7.2×10^{-10}	0.058	NO^+
$Ni^+ + NO + NO \rightarrow NiO^+ + N_2O$ (0.6) $\rightarrow NO^+ + NiNO$ (0.3) $\rightarrow NiNO^+ + NO$ (0.1)	1.5×10^{-11}	7.2×10^{-10}	0.021	
$Cu^+ + NO + NO \rightarrow NO^+ + CuNO$ (0.9) $\rightarrow CuNO^+ + NO$ (0.1)	6.8×10^{-12}	7.1×10^{-10}	9.2×10^{-3}	
$Zn^+ + NO \rightarrow NO^+ + Zn$ (0.97) $+ NO + NO \rightarrow ZnO^+$ (0.03)	1.0×10^{-10}	7.1×10^{-10}	0.14	
$Ga^+ + NO \rightarrow NR$	$\leq 6 \times 10^{-13}$	7.1×10^{-10}	$\leq 8 \times 10^{-4}$	
$Ge^+ + NO + NO \rightarrow NO^+ + GeNO$(0.6) $\rightarrow GeO^+ + N_2O$(0.4)	1.9×10^{-11}	7.1×10^{-10}	0.027	
$As^+ + NO \rightarrow NO^+ + As$	3.2×10^{-10}	7.0×10^{-10}	0.46	
$Se^+ + NO \rightarrow NO^+ + Se$	3.0×10^{-10}	6.9×10^{-10}	0.43	

[a] Product distributions are given in parentheses. The branching fractions are estimated to be accurate to ±20%. [b] Effective bimolecular rate coefficient first order in NO. The estimated uncertainty is ±30%. [c] Collision rate coefficient calculated using the algorithm of the modified variational transition-state/classical trajectory theory developed by Su and Chesnavich.[26]

endothermic.[24] So we can exclude formation of significant amounts of NO_2 and N_2O nitrogen oxides from reactions of NO with possible impurities such as H_2O or O_2 in the inlet system, which of course is continuously flushed with NO during a reaction measurement. There was also no indication of $(NO)_2^+$ formation from $(NO)_2$ dimer in any of the experiments. The known dissociation constant of $(NO)_2$ is 1.6×10^{23} molecules cm^{-3} at room temperature,[25] and this is large enough to keep the dimer concentration below 10^{-5}% of the monomer in the flow tube.

Reaction rate coefficients were determined in the usual manner.[19] Primary rate coefficients are determined from the observed semilogarithmic decay of the primary reactant ion intensity using pseudo-first-order kinetics. Higher-order rate coefficients are obtained by fitting the experimental data to the solutions of the system of differential equations for sequential reactions. These fits are shown in the graphical presentations of the experimental results. The rate coefficients for the primary and consecutive reactions reported herein have an absolute accuracy of ±30%. When rate coefficients are reported as an upper limit (≤), this indicates the statistical scatter in the data was significant compared to the slope of the data and an upper limit (based on the line of steepest slope through the data) is reported. Product distributions are obtained in the usual manner from plots of the fractional abundance of ions with added NO.

Results and Discussion

The reactions of 46 atomic ions with NO were investigated, including 29 transition-metal and 17 main-group cations. Some (seven) atomic ions were completely unreactive with NO in the dynamic range of our measurements, $k < 10^{-13}$ cm^3 $molecule^{-1}$ s^{-1}. These include the group 1 ions (K^+, Rb^+, Cs^+) that have a rare-gas configuration, the group 14 ions (In^+, Tl^+) that have a $d^{10}s^2$ filled-orbital configuration (Ga^+ was also quite unreactive), Pb^+ (s^2p^1) and Bi^+ (s^2p^2).

Two different channels, electron and O-atom transfer, were observed for bimolecular reactions known to be *exothermic* and these are indicated in reactions 2a and 2b, respectively.

$$X^+ + NO \rightarrow NO^+ + X \quad (2a)$$

$$\rightarrow XO^+ + N \quad (2b)$$

Competing N-atom transfer leading to the formation of XN^+, as has been reported for N^+ [13] and F^+,[14] was not observed in our experiments, presumably due to the lower stability of the XN^+ ions, viz. the nitrogen-atom affinity $NA(X^+) < NA(O) = 150.9 \pm 0.2$ kcal mol^{-1}.[11]

Unexpectedly, NO^+ and XO^+ product ions were often observed even when formation by bimolecular reaction first order in NO, reactions 2a and 2b, was *endothermic* for ground-state reactants. However, we realize that formation by termolecular reactions *second order in NO*, viz. Reactions 3 and 4, can often be exothermic. Exothermicity can be achieved in

$$X^+ + NO + NO \rightarrow NO^+ + X(NO) \quad (3)$$

$$X^+ + NO + NO \rightarrow XO^+ + N_2O \quad (4)$$

reactions 3 and 4 by bond formation in the neutral product: X−NO bond formation in reaction 3 and N−NO bond formation in reaction 4. Reaction 3 is exothermic when $IE(X) > IE(NO) - D(X-NO)$. Reaction 4 is exothermic when the oxygen-atom affinity $OA(X^+) > OA(N) - D(N-NO) = 36$ kcal mol^{-1}.[11] Remarkably, this is known to be the case, within experimental uncertainty, with 35 of the atomic ions investigated! Occasionally, $X^+(NO)$ also was observed to be produced with kinetics similar to reactions 3 and 4. We attribute this to the collisional stabilization with NO acting as the third body according to reaction 5. Because of its internal degrees of freedom, the NO

$$X^+ + NO + NO \rightarrow X^+(NO) + NO \quad (5)$$

TABLE 2: Rate Coefficients (cm^3 molecule^{-1} s^{-1}), Reaction Efficiencies (k/k_c), and Higher Order Product Ions Measured for Reactions of Second-Row Metal Cations with Nitric Oxide in Helium at 0.35 ± 0.01 Torr and 295 ± 2 K

reaction[a]	k[b]	k_c[c]	k/k_c	higher order product ions
$Rb^+ + NO \rightarrow NR$	$\leq 1 \times 10^{-13}$	6.8×10^{-10}	$\leq 10^{-4}$	
$Sr^+ + NO + NO \rightarrow SrO^+ + N_2O$	6.8×10^{-12}	6.8×10^{-10}	0.01	SrO_2^+, $SrO^+(NO)$, $SrO_2^+(NO)_{1,2}$
$Y^+ + NO \rightarrow YO^+ + N$	7.9×10^{-11}	6.8×10^{-10}	0.12	
$Zr^+ + NO \rightarrow ZrO^+ + N$	4.7×10^{-10}	6.8×10^{-10}	0.69	ZrO_2^+
$Nb^+ + NO \rightarrow NbO^+ + N$	4.7×10^{-10}	6.8×10^{-10}	0.69	NbO_2^+, NO^+
$Mo^+ + NO + NO \rightarrow MoO^+ + N_2O$ (0.5)	5.9×10^{-12}	6.7×10^{-10}	8.8×10^{-3}	
$\rightarrow NO^+ + MoNO$ (0.25)				
$\rightarrow MoNO^+ + NO$ (0.25)				
$Ru^+ + NO + NO \rightarrow RuO^+ + N_2O$	1.4×10^{-11}	6.7×10^{-10}	0.021	RuO_2^+, NO^+, $RuO^+(NO)_{1-3}$, $RuO_2^+(NO)_{1,2}$
$Rh^+ + NO + NO \rightarrow NO^+ + RhNO$ (0.7)	7.3×10^{-13}	6.7×10^{-10}	1.1×10^{-3}	
$\rightarrow RhNO^+ + NO$ (0.3)				$RhNO^+$ (NO)
$Pd^+ + NO + NO \rightarrow PdNO^+ + NO$ (0.45)	5.0×10^{-12}	6.7×10^{-10}	7.4×10^{-3}	
$\rightarrow NO^+ + PdNO$ (0.55)				
$Ag^+ + NO + NO \rightarrow NO^+ + AgNO$	9.4×10^{-13}	6.7×10^{-10}	1.4×10^{-3}	
$Cd^+ + NO + NO \rightarrow NO^+ + CdNO$	1.7×10^{-12}	6.6×10^{-10}	2.6×10^{-3}	
$In^+ + NO \rightarrow NR$	$\leq 1 \times 10^{-13}$	6.6×10^{-10}	$\leq 10^{-4}$	
$Sn^+ + NO + NO \rightarrow NO^+ + SnNO$ (0.9)	2.1×10^{-11}	6.5×10^{-10}	0.032	
$\rightarrow SnO^+ + N_2O$ (0.1)				
$Sb^+ + NO + NO \rightarrow NO^+ + SbNO$ (0.15)	2.7×10^{-11}	6.5×10^{-10}	4.2×10^{-2}	
$\rightarrow SbO^+ + N_2O$ (0.85)				
$Te^+ + NO + NO \rightarrow NO^+ + TeNO$ (0.5)	1.9×10^{-12}	6.5×10^{-10}	2.9×10^{-3}	
$\rightarrow TeO^+ + N_2O$ (0.5)				

[a] Product distributions are given in parentheses. The branching fractions are estimated to be accurate to ±20%. [b] Effective bimolecular rate coefficient first order in NO. The estimated uncertainty is ±30%. [c] Collision rate coefficient calculated using the algorithm of the modified variational transition-state/classical trajectory theory developed by Su and Chesnavich.[26]

TABLE 3: Rate Coefficients (cm^3 molecule^{-1} s^{-1}), Reaction Efficiencies (k/k_c), and Higher Order Product Ions Measured for Reactions of Third-Row Metal Cations with Nitric Oxide in Helium at 0.35 ± 0.01 Torr and 295 ± 2 K

reaction[a]	k[b]	k_c[c]	k/k_c	higher order product ions
$Cs^+ + NO \rightarrow NR$	$\leq 1 \times 10^{-13}$	6.6×10^{-10}	$\leq 10^{-4}$	
$Ba^+ + NO + NO \rightarrow BaO^+ + N_2O$	2.1×10^{-11}	6.5×10^{-10}	0.032	BaO_2^+, NO^+
$La^+ + NO \rightarrow LaO^+ + N$	2.6×10^{-10}	6.5×10^{-10}	0.40	
$Hf^+ + NO \rightarrow HfO^+ + N$	5.6×10^{-10}	6.5×10^{-10}	0.87	HfO_2^+, NO^+
$Ta^+ + NO \rightarrow TaO^+ + N$	5.7×10^{-10}	6.4×10^{-10}	0.89	TaO_2^+, NO^+
$W^+ + NO \rightarrow WO^+ + N$	5.0×10^{-10}	6.3×10^{-10}	0.79	$WO_{2,3}^+$, NO^+
$Re^+ + NO + NO \rightarrow ReO^+ + N_2O$	1.3×10^{-11}	6.3×10^{-10}	0.021	ReO_{2-4}^+, NO^+
$Os^+ + NO + NO \rightarrow OsO^+ + N_2O$	1.5×10^{-11}	6.3×10^{-10}	0.024	OsO_2^+, NO^+, $OsO^+(NO)_{1-3}$
$Ir^+ + NO + NO \rightarrow IrO^+ + N_2O$ (0.95)	1.5×10^{-11}	6.3×10^{-10}	0.024	NO^+, $IrO^+(NO)$
$\rightarrow IrNO^+ + NO$(0.05)				$IrNO^+(NO)$
$Pt^+ + NO + NO \rightarrow NO^+ + PtNO$ (0.9)	1.2×10^{-11}	6.3×10^{-10}	0.019	
$\rightarrow PtNO^+ + NO$ (0.1)				$Pt^+(NO)_{2,3}$
$Au^+ + NO \rightarrow NO^+ + Au$	1.0×10^{-10}	6.3×10^{-10}	0.16	
$Hg^+ + NO \rightarrow NO^+ + Hg$	1.2×10^{-10}	6.3×10^{-10}	0.19	
$Tl^+ + NO \rightarrow NR$	$\leq 1 \times 10^{-13}$	6.3×10^{-10}	$\leq 10^{-4}$	
$Pb^+ + NO \rightarrow NR$	$\leq 1 \times 10^{-13}$	6.3×10^{-10}	$\leq 10^{-4}$	
$Bi^+ + NO \rightarrow NR$	$\leq 1 \times 10^{-13}$	6.3×10^{-10}	$\leq 10^{-4}$	

[a] Product distributions are given in parentheses. The branching fractions are estimated to be accurate to ±20%. [b] Effective bimolecular rate coefficient first order in NO. The estimated uncertainty is ±30%. [c] Collision rate coefficient calculated using the algorithm of the modified variational transition-state/classical trajectory theory developed by Su and Chesnavich.[26]

molecule is expected to be a better third body than the He atom in stabilizing the intermediate $(X^+,NO)^*$.

The kinetic results of our experiments are summarized in Tables 1−3 according to row in the periodic table. The tabulated *effective* bimolecular rate coefficients, k, apply either to exothermic bimolecular reactions of type (2a) or (2b) that are first order in NO or to exothermic termolecular reactions of type (3), (4), or (5) that are second order in NO. Ions produced by further reactions with NO are included in the listing of higher order product ions, i.e., the right-hand column, in Tables 1−3. Also included are calculated reaction efficiencies expressed as k/k_c. The collision rate coefficients, k_c, are calculated using the algorithm of the modified variational transition-state/classical trajectory theory developed by Su and Chesnavich[26a] with α-(NO) = 1.70×10^{-24} cm^3 and μ_D = 0.161 D.[26b]

Bimolecular Transfer Reactions. The kinetic results for the observed bimolecular electron transfer and O-atom transfer reactions are displayed on a periodic table in Figure 1.

Bimolecular Electron Transfer. Bimolecular electron transfer, reaction 2a, is exothermic and was observed for those three transition-metal ions (Zn^+, Au^+, Hg^+) and two main-group ions (As^+, Se^+) with IE (X) ≥ IE (NO) = 9.26436 ± 0.00006 eV[11] (see Table 4). Figure 2 shows results obtained with Zn^+. The electron transfer between Au^+ (with IE = 9.225 eV)[11] and NO is essentially thermoneutral (ΔIE = 0.03 eV). Figure 3 shows how the efficiency for electron transfer varies with IE (M^+). For the most part, these electron transfer reactions are fairly rapid when exothermic with k = 0.97, 3.2, 3.0, and 1.2×10^{-10} cm^3 molecule^{-1} s^{-1} but do not have unit efficiency with k/k_c = 0.14, 0.46, 0.43, and 0.19 for Zn^+, As^+, Se^+, and Hg^+,

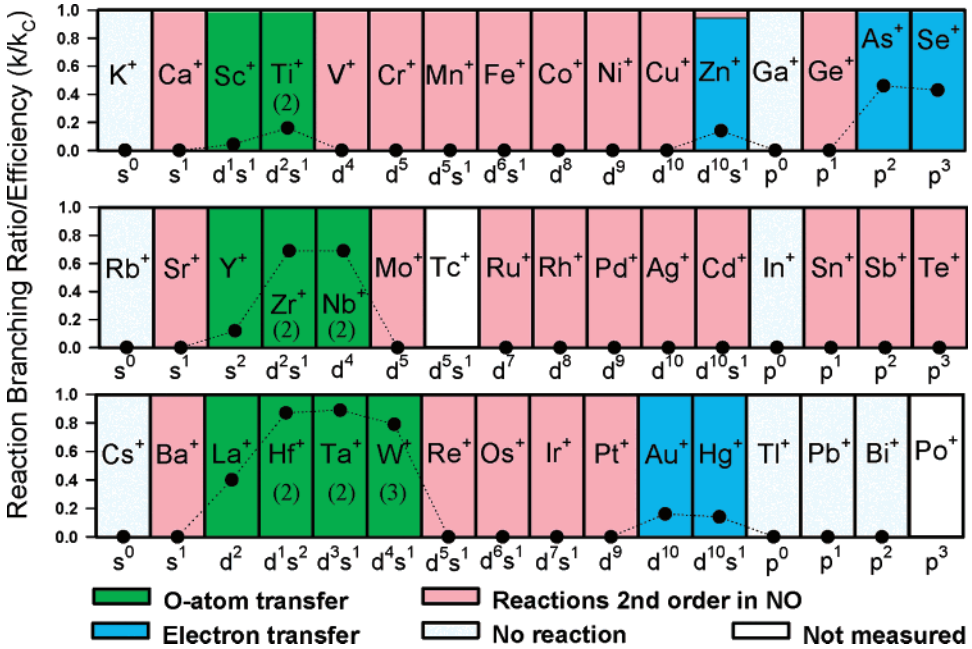

Figure 1. Periodic variations observed in the efficiencies, k/k_c (represented as solid circles), for reactions of nitric oxide with transition-metal ions and main-group cations. k represents the measured reaction rate coefficient, and k_c is the calculated collision rate coefficient (see Tables 1−3). Also indicated are the observed reaction channels and the ground-state electronic configurations of the atomic cations. The reactions of Tc^+ and Po^+ were not investigated. The numbers in parentheses indicate the number of observed sequential O-atom transfer reactions.

TABLE 4: O-Atom Affinities, $D_0(M^+-O)$ in kcal mol^{-1}, and Ionization Energies, IE(M) in eV, for the Transition-Metal Ions Taken, with Few Exceptions, from the Review by Schröder et al.[28]

first row			second row			third row		
M^+	$OA(M^+)$	IE(M)	M^+	$OA(M^+)$	IE(M)	M^+	$OA(M^+)$	IE(M)
K^+	3	4.34	Rb^+	7	4.18	Cs^+	14	3.89
Ca^+	77.2	6.11	Sr^+	71.4	5.70	Ba^+	92.8	5.21
Sc^+	164.6 ± 1.4[a]	6.56	Y^+	167.0 ± 4.2[b]	6.22	La^+	206 ± 4[d]	5.58
Ti^+	158.6 ± 1.6[a]	6.83	Zr^+	178.9 ± 2.5[b]	6.63	Hf^+	173 ± 5[e]	6.83
V^+	134.9 ± 3.5[a]	6.75	Nb^+	164.4 ± 2.5[b]	6.76	Ta^+	188 ± 15[e]	7.55
Cr^+	85.8 ± 2.8[a]	6.77	Mo^+	116.7 ± 0.5[b]	7.09	W^+	166 ± 10[f]	7.86
Mn^+	68.0 ± 3.0[a]	7.43				Re^+	115 ± 15[g]	7.83
Fe^+	80.0 ± 1.4[a]	7.90	Ru^+	87.9 ± 1.2[c]	7.36	Os^+	100 ± 12[h]	8.44
Co^+	74.9 ± 1.2[a]	7.88	Rh^+	69.6 ± 1.4[c]	7.46	Ir^+	59[e]	8.97
Ni^+	63.2 ± 1.2[a]	7.64	Pd^+	33.7 ± 2.5[c]	8.34	Pt^+	77,[i] 75 ± 2[j]	8.96
Cu^+	37.4 ± 3.5[a]	7.72	Ag^+	28.4 ± 1.2[c]	7.58	Au^+		9.23
Zn^+	38.5 ± 1.2[a]	9.39	Cd^+		8.99	Hg^+		10.44
Ga^+	5.6	6.00	In^+		5.79	Tl^+		6.11
Ge^+	81.8	7.90	Sn^+	75.1	7.34	Pb^+	53.2	7.42
As^+	147 ± 2[k]	9.81	Sb^+		8.64	Bi^+	41.6	7.29
Se^+	92[k]	9.75	Te^+	96.6	9.01			

[a] Reference 29. [b] Reference 30. [c] Reference 31. [d] Reference 32. [e] Reference 11. [f] Reference 33. [g] Reference 34. [h] Reference 35. [i] Reference 36. [j] Reference 37. [k] Reference 38.

respectively. We have reported separately the extent to which energy resonance and Franck−Condon factors may be responsible for determining the magnitudes of these electron transfer efficiencies.[27]

Bimolecular O-Atom Transfer. Figure 4 provides measured profiles for the O-atom transfer reactions of Ti^+, Zr^+, Nb^+, and Ta^+ with NO and Figure 3 shows how the efficiency for O-atom transfer varies with OA (X^+). The bimolecular O-atom transfer channel (1b) is exothermic and was observed for those nine transition-metal ions (Sc^+, Ti^+, Y^+, Zr^+, Nb^+, La^+, Hf^+, Ta^+, W^+) for which OA (X^+) > OA (N) = 150.9 ± 0.2 kcal mol^{-1},[11] (see Table 4). Our results for Ti^+ and Zr^+ with $k = (1.2 \pm 0.4) \times 10^{-10}$ and $(4.7 \pm 1.4) \times 10^{-10}$ cm^3 molecule^{-1} s^{-1}, respectively, are in good agreement with the previously reported room-temperature values of $(9.5 \pm 2) \times 10^{-11}$ and $(4.8 \pm 0.6) \times 10^{-10}$ cm^3 molecule^{-1} s^{-1} obtained using a selected-ion drift apparatus coupled to a hot-filament and ion-discharge source, respectively.[15,16] There is also agreement with the early qualitative ICR results that indicated oxidation with Ti^+, Zr^+, and Nb^+ but not with V^+.[17]

Termolecular Reactions. Of the 46 atomic ions investigated, 14 react with NO in an exothermic bimolecular fashion: 5 by direct electron transfer, reaction 2a, and 9 by O-atom transfer, reaction 2b. Of the remaining 32 atomic ions, all but 8 appeared to react in termolecular reactions of type (3a), (3b), or (5) that are second order in NO. The remaining 8 are totally unreactive (K^+, Rb^+, Cs^+, Ga^+, In^+, Tl^+, Pb^+ and Bi^+).

Termolecular XO^+ Formation. Reaction 4 is exothermic when $OA(X^+) > OA(N) - D(N-NO) = 36$ kcal mol^{-1}, and this is the case for almost all of the atomic ions investigated except for $X^+ = K^+$, Rb^+, Pd^+, Cs^+, Ag^+, and Ga^+ (see Table 4) and probably also Cd^+, In^+, and Tl^+, whose O-atom affinities, although not known, are likely to be lower than 36 kcal mol^{-1} based on the low values for $OA(Zn^+)$ and $OA(Ga^+)$. Figure 5

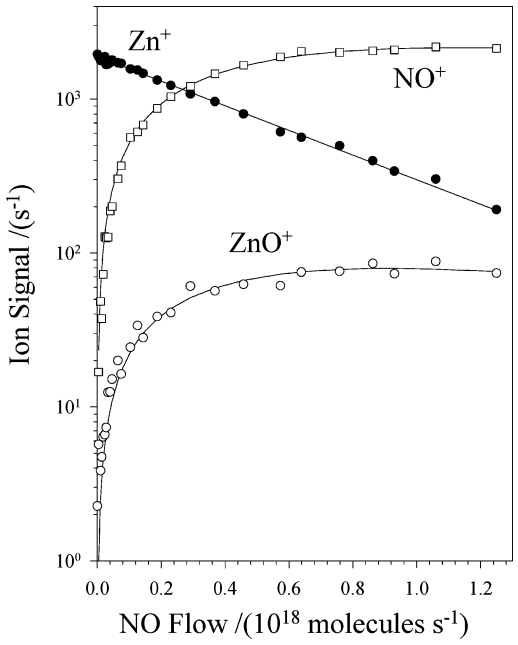

Figure 2. ICP/SIFT results for the reaction of Zn^+ with nitric oxide in helium buffer gas at 0.35 ± 0.01 Torr and 295 ± 2 K.

provides measured profiles for the reactions of V^+, Fe^+, Ru^+, and Os^+ that exhibit XO^+ formation that is expected to be second order in NO.

All of the first-row cations for which direct O-atom transfer is endothermic exhibit XO^+ formation except for K^+ (s^0) and Ga^+ (p^0) that do not react at all and Cu^+ (d^{10}) that forms mainly NO^+ (0.9) and some $CuNO^+$ (0.1).

All of the second-row cations for which direct O-atom transfer is endothermic exhibit XO^+ formation except for Rb^+ (s^0) that does not react at all, Rh^+ (d^8) and Pb^+ (d^9) that form NO^+ and X^+ (NO), Ag^+ (d^{10}) and Cd^+ ($d^{10}s^1$) that slowly form NO^+, and In^+ (p^0) that is unreactive.

Only four third-row cations (Ba^+, Re^+, Os^+, Ir^+) for which direct O-atom transfer is endothermic exhibit XO^+ formation. The others exhibit direct exothermic O-atom transfer (La^+, Hf^+, Ta^+, W^+), exothermic electron transfer (Au^+, Hg^+), or no reaction (Cs^+ (s^0), Tl^+(p^0), Pb^+ (p^1), Bi^+ (p^2)). Pt^+ (d^9) is the only third-row cation that exhibits NO^+ formation even though direct electron transfer is endothermic.

Exclusive XO^+ formation was observed with the group 2 (s^1) cations Ca^+, Sr^+, and Ba^+, with the group 8 cations Fe^+ (d^6s^1), Ru^+ (d^7), and Os^+ (d^6s^1), with the group 7 cation Re^+ (d^5s^1), and with the group 9 cation Co^+ (d^8).

Termolecular NO^+ Formation. Reaction 3 is exothermic when IE(X) > IE(NO) − D(X−NO) or 9.264 eV − D_{298}(X−NO). The bond energies D_{298}(X−NO) are generally unknown, but density-functional calculations of mononitrosyls of first-row transition-metal atoms have provided binding energies, D_e(X−NO), that decrease from Sc at 2.5 eV to Ni and Cu at about 1.3 eV, remaining almost constant at almost 2.2 eV between Ti and Fe and has a value of 2.0 eV for Co.[39] These values would make NO^+ formation by reaction 3a exothermic for $X^+ = Mn^+$, Fe^+, and Co^+ and endothermic by at least 0.2 eV for Sc^+ and at least 0.3 eV for $X^+ = V^+$, Cr^+, Ni^+, and Cu^+ because $D_e > D_{298}$. The value of D_0(Ga−NO) = 1.6 eV computed at the B3LYP/6-311+G(d) level[40] makes reaction 3a with Ga^+ endothermic by 1.7 eV. Figure 6 provides measured profiles for the reactions of Cu^+, Pd^+, Sn^+, and Pt^+ that exhibit NO^+ formation that is expected to be second order in NO.

Five of the first-row atomic cations (Cr^+, Mn^+, Ni^+, Cu^+, Ge^+) appear to exhibit primary NO^+ formation second order in NO. However, NO^+ formation always occurs in competition with another channel (see Table 1): formation of $XO^+ + N_2O$ (reaction b in the case of Cr^+, Mn^+, Ni^+, and Ge^+ and formation of X^+(NO) + NO (reaction c) in the case of Cu^+. The computed metal−nitrosyl binding energies predict exothermicity only for the reaction with Mn^+. NO^+ also was observed in the chemistry initiated by V^+, Fe^+ (see Figure 5), and Co^+, but product-ion ratio analyses indicate secondary formation of NO^+ either by reaction 6, also second order in NO, or by reaction 7, electron transfer from NO to the primary XO^+ product (which may be formed with some internal energy).

$$XO^+ + NO + NO \rightarrow NO^+ + XNO_2 \quad (6)$$

$$XO^+ + NO \rightarrow NO^+ + XO \quad (7)$$

In the case of V^+ for example (see Figure 7), the product-ion ratio analysis indicates the occurrence of reaction 8 in the

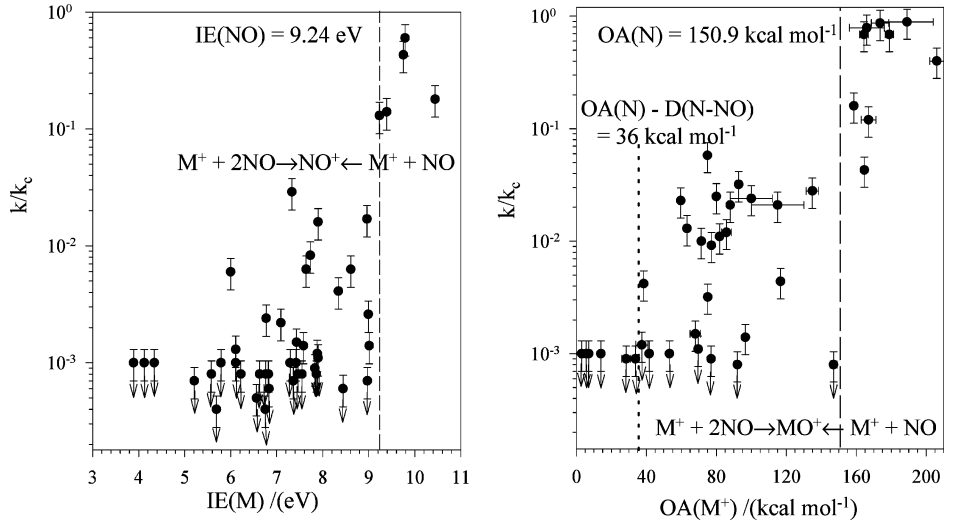

Figure 3. Semilogarithmic dependence of the efficiency, k/k_c, for NO^+ formation on the ionization energy, IE(M), and MO^+ formation on the O-atom affinity, OA(M^+), in reactions of atomic cations with nitric oxide. k represents the measured first-order or pseudo-first-order reaction rate coefficient, and k_c is the calculated collision rate coefficient (see Table 1). Bimolecular electron transfer and O-atom transfer reactions are exothermic on the right of the dashed lines and endothermic on the left. Termolecular MO^+ formation is exothermic to the right of the dotted line.

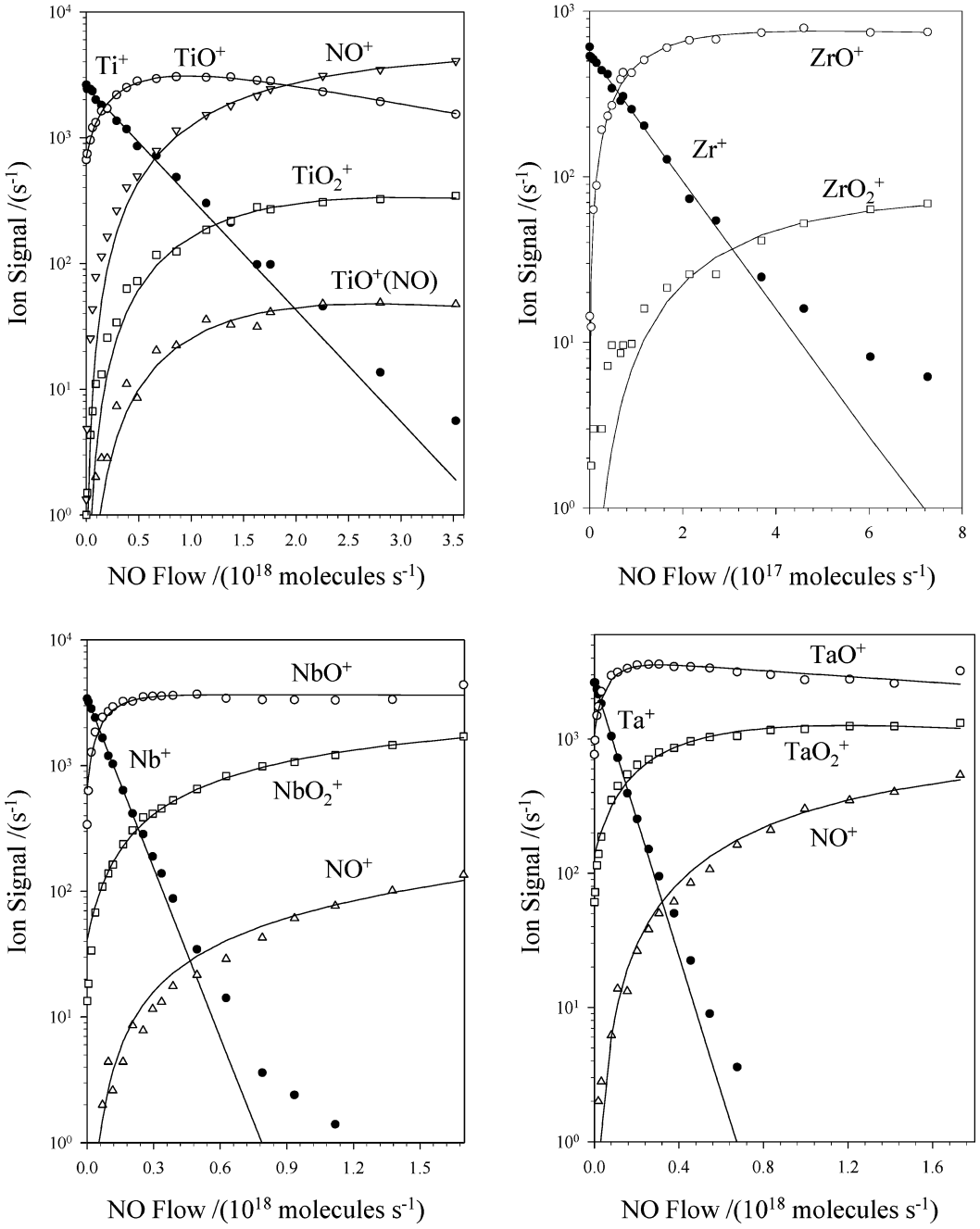

Figure 4. Composite of ICP/SIFT results for bimolecular O-atom transfer reactions (first order in NO) of nitric oxide with atomic cations in helium buffer gas at 0.35 ± 0.01 Torr and 295 ± 2 K.

ratio (8a)/(8b)/(8c) = 0.7/0.3/0.1. Further production of NO^+ occurs by the reaction of VO_2^+ with NO. There has been one

$$VO^+ + NO + NO \rightarrow VO_2^+ + N_2O \quad (8a)$$

$$\rightarrow NO^+ + VNO_2 \quad (8b)$$

$$\rightarrow VO^+(NO) + NO \quad (8c)$$

previous report of rapid NO^+ formation with Fe^+ (close to the collision rate), but this was attributed to the reaction of excited states of $(Fe^+)^*$ that lie at least 1.31 eV above the ^6D ground state.[41] The ground state was reported to be unreactive with NO. This latter result is perhaps not surprising because these experiments were performed with FT-ICR mass spectrometry at lower concentrations of NO.

Six of the second-row atomic cations (Mo^+, Rh^+, Pd^+, Sn^+, Sb^+, Te^+) appear to exhibit primary NO^+ formation second order in NO. In all cases, however, it occurs again in competition with other channels (see Table 2). The NO^+ observed in the chemistry initiated by Nb^+ and Ru^+ is attributed to further reactions of the oxide cations.

Only one of the third-row atomic cations (Pt^+) appears to exhibit primary NO^+ formation second order in NO, in this case in competion with formation of $PtNO^+ + NO$. The NO^+ observed in the chemistry initiated by Ba^+, Hf^+, Ta^+, W^+, Re^+, Os^+, and Ir^+ is attributed to further reactions of the oxide cations.

Termolecular $X^+(NO)$ Formation. Reaction 5 is exothermic for the X^+ ions investigated here, all of which are expected to have a positive affinity for NO, but must compete with (3) and (4). Molecular NO is expected to be more effective than a He atom in the collisional deactivation of $(X^+,NO)^*$ formed in reaction 5. However, the collisional deactivation of $(X^+,NO)^*$ by NO must compete with the reaction which leads to NO^+

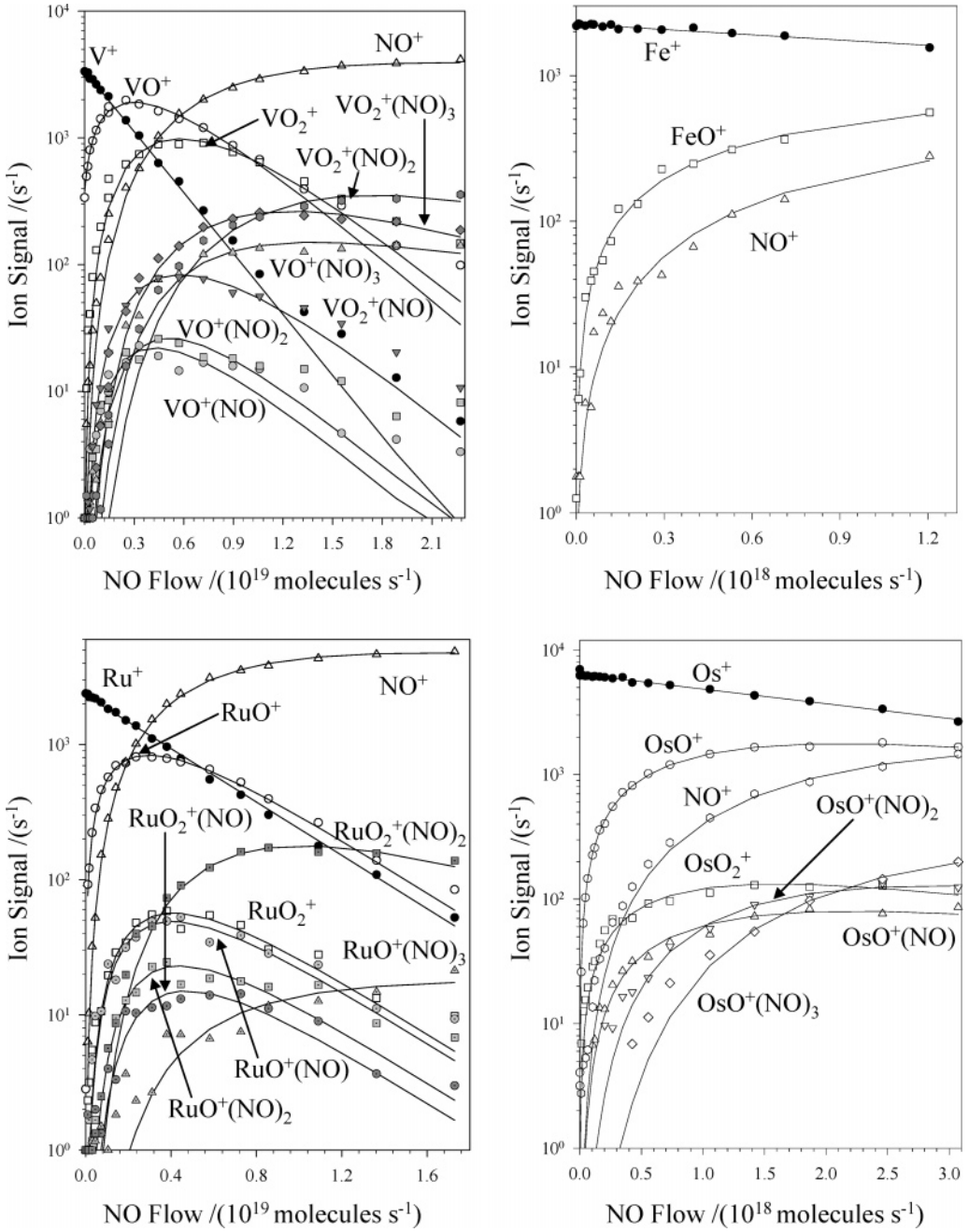

Figure 5. Composite of ICP/SIFT results for termolecular formation of XO^+ (second order in NO) and NO ligation in reactions of nitric oxide with atomic cations in helium buffer gas at 0.35 ± 0.01 Torr and 295 ± 2 K.

and (X,NO), especially if the latter is more exothermic, viz. if IE (X,NO) > IE(NO).

An inspection of the observed product ions indicates that formation of X^+(NO) is much less common than formation of (X,NO). Thus minor channels leading to X^+(NO) formation were recorded for X = Ni and Cu (first row), X = Mo, Rh, and Pd (second row), and X = Ir and Pt (third row). In all these cases except Ir, (X,NO) + NO^+ formation was predominant or at least equal to X^+(NO) formation. IrO^+ formation was predominant with Ir. Furthermore, XNO formation was observed with X = Cr and Mn (first row) and with X = Ag, Cd, Sn, Sb, and Te (second row). No (X,NO) formation was apparent with the third-row atomic cations.

As far as we are aware, most of these X^+(NO) cations have not been seen before. Mass spectrometric evidence for $CuNO^+$ was first reported in 1991.[42] It was formed by electron impact ionization (70 eV) of anhydrous copper nitrate. More recent experiments have demonstrated the formation of $CuNO^+$ by the association reaction of NO to Cu^+ produced by Ar^+-sputtering from a copper cathode.[43] Also, a bond strength of $D_0(Cu^+-NO)$ = 1.13 ± 0.08 eV was determined by means of guided ion beam mass spectrometry and the $CuNO^+$ isomer was shown with calculations to be 0.4 eV more stable than the $CuON^+$ isomer.[43] $NiNO^+$ also has been observed previously and was produced by ligating Ni^+ with NO in a dc discharge source.[44] $CuNO^+$ and $ZnNO^+$ have been produced previously from reactions of NO_2 with Cu^+ and Zn^+ respectively, in a guided ion-beam mass spectrometer.[45]

Overview of Second-Order NO Chemistry. The identification of the ion chemistry that is second order in NO is an important new result that has implications for NO chemistry generally in any environment that is rich in NO. The second-order reactions with many of the ground-state atomic cations that are investigated here clearly are thermodynamically favored

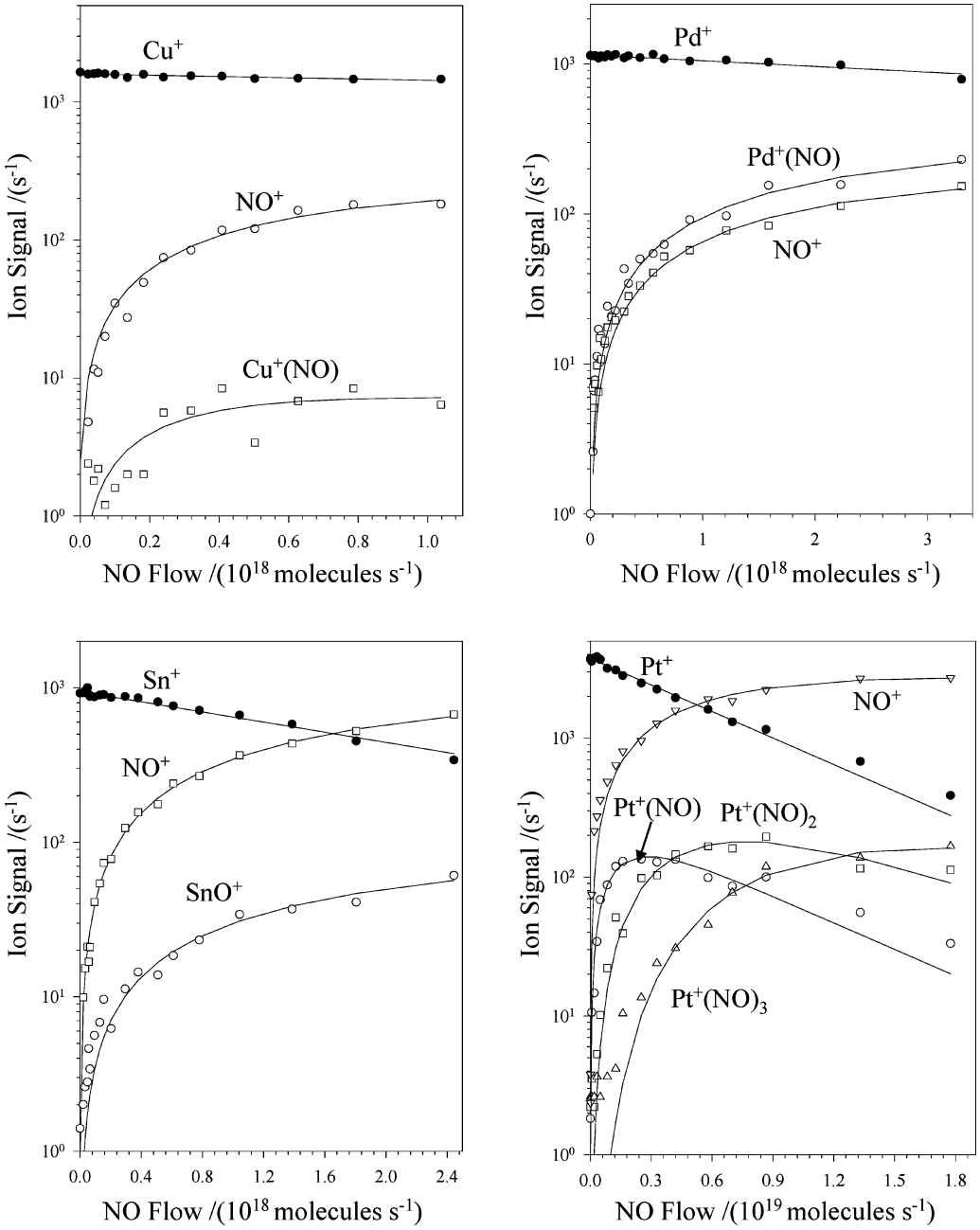

Figure 6. Composite of ICP/SIFT results for termolecular formation of NO^+ (second order in NO) and NO ligation in reactions of nitric oxide with atomic cations in helium buffer gas at 0.35 ± 0.01 Torr and 295 ± 2 K.

to produce MO^+ and, but less so, NO^+ ions that are not accessible to first-order NO chemistry. Unfortunately, the observed first- and second-order kinetics could not be distinguished on the basis of the observed shape of the M^+ decay. There is a general difference in the apparent reaction rate: the reactions first order in NO have efficiencies generally >0.1, whereas the reactions second order in NO have apparent efficiencies generally <0.06.

The low apparent rate coefficients and efficiencies of the reactions second order in NO, reactions 3−5, can be understood in terms of a two-step mechanism involving the formation of a temporary adduct ion $(X^+,NO)^*$, reaction 9, as a first step.

$$X^+ + NO \rightarrow (X^+,NO^+)^* \qquad (9)$$

At high flows of NO this intermediate is more likely to encounter another NO molecule and this can result in formation of NO^+, XO^+ and XNO^+ via reactions 10a−10c. Also, a

$$(X^+,NO)^* + NO \rightarrow NO^+ + (X,NO) \qquad (10a)$$

$$(X^+,NO)^* + NO \rightarrow XO^+ + N_2O \qquad (10b)$$

$$(X^+,NO)^* + NO \rightarrow X^+(NO) + NO \qquad (10c)$$

fraction of the intermediate may be dissociated according to reaction 10d.

$$(X^+,NO)^* + NO \rightarrow X^+ + 2NO \qquad (10d)$$

Figure 7 shows kinetic simulations using this mechanism for two cases with small apparent rate coefficients of 7.7×10^{-11} and 8.6×10^{-12} cm^3 molecule^{-1} s^{-1}, both of which lead to linearity in the semilogarithmic decay of X^+. These results illustrate a possible origin of linearity in the primary ion decay

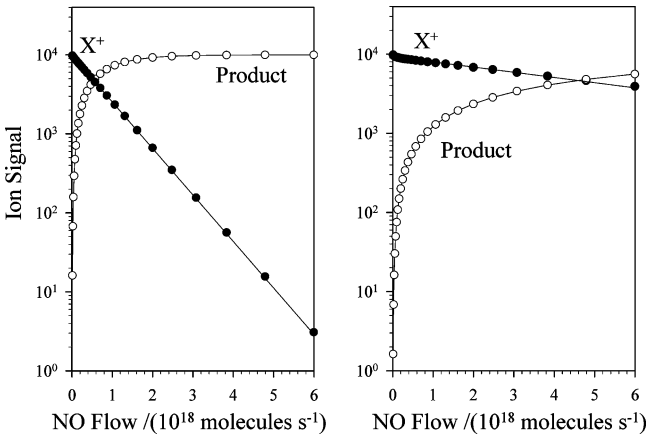

Figure 7. Simulated profiles for the second-order reaction of X^+ and NO. LHS: $k_9 = 7.5 \times 10^{-10}$ cm^3 molecule^{-1} s^{-1}, $k_{-9} = 50$ s^{-1}, $k_{10a,b,c} = 1 \times 10^{-10}$ cm^3 molecule^{-1} s^{-1}, $k_{10d} = 6.5 \times 10^{-10}$ cm^3 molecule^{-1} s^{-1} and an apparent bimolecular arte coefficient of 7.7×10^{-11} cm^3 molecule^{-1} s^{-1}. RHS: $k_9 = 7.5 \times 10^{-10}$ cm^3 molecule^{-1} s^{-1}, $k_{-9} = 50$ s^{-1}, $k_{10a,b,c} = 1 \times 10^{-11}$ cm^3 molecule^{-1} s^{-1}, $k_{10d} = 6.5 \times 10^{-10}$ cm^3 molecule^{-1} s^{-1} and an apparent bimolecular rate coefficient of 8.6×10^{-12} cm^3 molecule^{-1} s^{-1}.

for a reaction second order in NO and so the difficulty in distinguishing second from first order (in NO) kinetics from the shape of the measured primary ion decay. The low apparent rate coefficients can be attributed mainly to rapid dissociation of the temporary adduct ion $(X^+,NO)^*$ by NO, reaction 7d.

The kinetic results for the second-order chemistry with NO are displayed on the periodic table shown in Figure 8. Both the variations in reaction efficiency and the variations in product distributions exhibit some periodic behavior. When exothermic, XO^+ formation is favored for atomic ions with s^1 and d^ns^1 configurations, although it competes with second-order NO^+ formation in the case of Mn^+ and first-order electron transfer in the case of Zn^+.

Higher Order Multiple Oxide Formation and NO Ligation. Tables 1−3 list the higher order product ions that were observed and Table 5 indicates the reactions that are proposed to lead to these ions, together with rate coefficients for those reactions for which they were accessible. Dioxide and, in the case of W and Re, multiple oxide formation as well as NO ligation were the main higher order reactions that were observed.

Dioxide cation formation can proceed either by bimolecular O-atom transfer to the monoxide cation, reaction 11, which is first order in NO, or by the termolecular reaction 10 that is second order in NO. For reaction 11 to be exothermic with

$$XO^+ + NO \rightarrow XO_2^+ + N \qquad (11)$$

$$XO^+ + NO + NO \rightarrow XO_2^+ + N_2O \qquad (12)$$

thermalized XO^+ ions, $OA(XO^+)$ must exceed $OA(N) = 150.9 \pm 0.2$ kcal mol^{-1}.[11] Reaction 12 is 115 kcal mol^{-1} more exothermic than reaction 11 because it leads to the formation of the N−NO bond and so is thermodynamically more favorable.

None of the known O-atom affinities of XO^+ exceed 151 kcal mol^{-1}.[27] The reported values for the O-atom affinities (in kcal mol^{-1}) of the first-row oxide cations are ScO^+ (40), TiO^+ (81), VO^+ (90), CrO^+ (66), FeO^+ (66), and CuO^+ (99). Those for the second-row oxide cations are YO^+ (41), ZrO^+ (89), NbO^+ (132), MoO^+ (128), RuO^+ (79), and RhO^+ (78) whereas those for the third-row oxide cations are LaO^+ (23), TaO^+ (140), WO^+ (132), ReO^+ (65), OsO^+ (105), IrO^+ (125), and PtO^+ (75). The least endothermic O-atom transfer reaction of any of these oxide cations is that with TaO^+ which still is endothermic by 11 kcal mol^{-1}. In our measurements we have observed dioxide cation formation with CaO^+, TiO^+, VO^+, and CrO^+, with SrO^+, ZrO^+, NbO^+, and RuO^+, and with BaO^+, HfO^+, TaO^+, WO^+, ReO^+, and OsO^+. Of these, dioxide formation from monoxide cations reacting with NO have been reported only for TiO^+ and ZrO^+.[15,16]

We propose that the plethora of dioxide formation observed in our experiments (see Tables 1−3) is predominantly due to the termolecular reaction 12, which is second order in NO. In the unlikely event that some of the exothermicity of the reactions (either first or second order in NO) leading to XO^+ formation is retained before collision with another NO molecule, we cannot

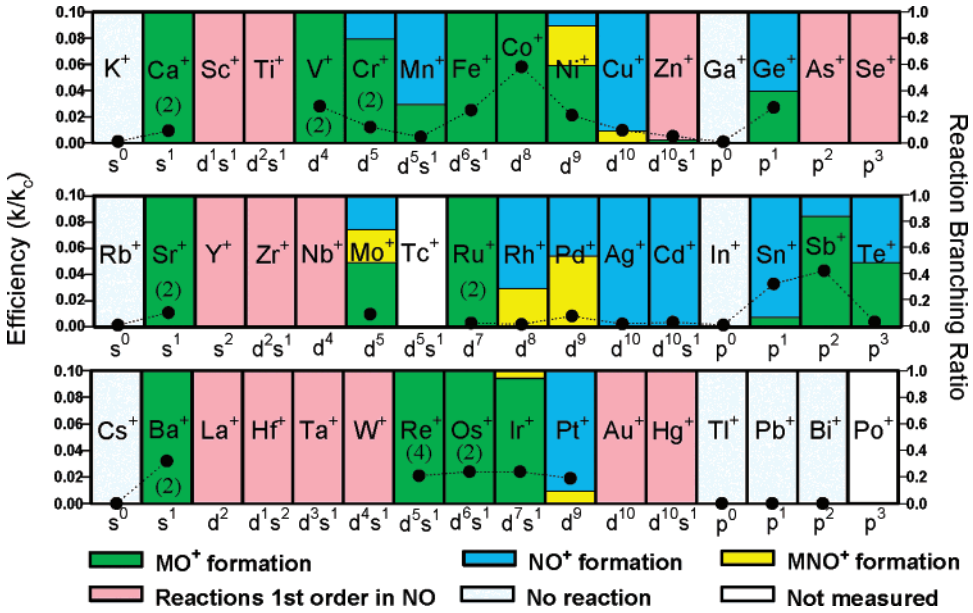

Figure 8. Periodic variations observed in the efficiencies, k/k_c (represented as solid circles), for second-order reactions of nitric oxide with transition-metal ions and main-group cations. k represents the measured effective bimolecular reaction rate coefficient and k_c is the calculated collision rate coefficient (see Tables 1−3). Also indicated are the observed reaction channels and the ground-state electronic configurations of the atomic cations. The reactions of Tc^+ and Po^+ were not investigated. The numbers in parentheses indicate the number of observed sequential MO^+ formation reactions.

TABLE 5: Rate Coefficients (k, cm^3 molecule^{-1} s^{-1}) and Product Distributions Measured for Reactions between Oxide Cations and Nitric Oxide in Helium at 0.35 ± 0.01 Torr and 295 ± 2 K

reaction	product distribution[a]	k[b]
$CaO^+ + 2\,NO \rightarrow CaO_2^+ + N_2O$	0.5	3.5×10^{-12}
$\rightarrow CaO^+(NO) + NO$	0.5	
$ScO^+ + NO \rightarrow ScO^+(NO)$	1	$\leq 7 \times 10^{-12}$
$TiO^+ + 2\,NO \rightarrow NO^+ + TiONO$	0.83	2.0×10^{-11}
$\rightarrow TiO_2^+ + N_2O$	0.13	
$\rightarrow TiO^+(NO) + NO$	0.02	
$VO^+ + 2\,NO \rightarrow VO_2^+ + N_2O$	0.67	1.5×10^{-11}
$\rightarrow NO^+ + VNO$	0.27	
$\rightarrow VO^+(NO) + NO$	0.06	
$VO^+(NO) + NO \rightarrow VO^+(NO)_2$	1	observed
$VO^+(NO)_2 + NO \rightarrow VO^+(NO)_3$	1	observed
$VO_2^+ + NO \rightarrow VO_2^+(NO)$	1	observed
$VO_2^+(NO) + NO \rightarrow VO_2^+(NO)_2$	1	observed
$VO_2^+(NO)_2 + NO \rightarrow VO_2^+(NO)_3$	1	observed
$CrO^+ + 2\,NO \rightarrow CrO_2^+ + N_2O$	1	$\leq 1.8 \times 10^{-11}$
$FeO^+ + 2\,NO \rightarrow NO^+ + FeONO$	1	$\leq 3.4 \times 10^{-11}$
$CoO^+ + 2\,NO \rightarrow NO^+ + CoONO$	1	$\leq 3.5 \times 10^{-11}$
$SrO^+ + 2\,NO \rightarrow SrO_2^+ + N_2O$	0.80	$\leq 6.4 \times 10^{-12}$
$\rightarrow SrO^+(NO) + NO$	0.20	
$SrO_2^+ + NO \rightarrow SrO_2^+(NO)$	1	$\leq 1.0 \times 10^{-11}$
$SrO_2^+ + NO \rightarrow SrO_2^+(NO)_2$	1	observed
$ZrO^+ + 2\,NO \rightarrow ZrO_2^+ + N_2O$	1	$\leq 6.2 \times 10^{-12}$
$NbO^+ + 2\,NO \rightarrow NbO_2^+ + N_2O$	1	$\leq 4.4 \times 10^{-11}$
$NbO_2^+ + NO \rightarrow NO^+ + NbO_2$	1	observed
$RuO^+ + 2\,NO \rightarrow NO^+ + RuONO$	0.6	2.8×10^{-11}
$\rightarrow RuO_2^+ + N_2O$	0.2	
$\rightarrow RuO^+(NO) + NO$	0.2	
$RuO^+(NO) + NO \rightarrow RuO^+(NO)_2$	1	$\leq 6.5 \times 10^{-11}$
$RuO^+(NO)_2 + NO \rightarrow RuO^+(NO)_3$	1	$\leq 1.1 \times 10^{-10}$
$RuO_2^+ + NO \rightarrow RuO_2^+(NO)$	1	$\leq 6.8 \times 10^{-11}$
$RuO_2^+(NO) + NO \rightarrow RuO_2^+(NO)_2$	1	$\leq 1.8 \times 10^{-10}$
$Rh^+(NO) + NO \rightarrow Rh^+(NO)_2$	1	observed
$TeO^+ + NO + NO \rightarrow NO^+ + TeONO$	1	observed
$BaO^+ + NO + NO \rightarrow BaO_2^+ + N_2O$	1	$\leq 1.4 \times 10^{-11}$
$BaO_2^+ + NO \rightarrow NO^+ + BaO_2$	1	observed
$HfO^+ + 2\,NO \rightarrow HfO_2^+ + N_2O$	0.85	$\leq 1.8 \times 10^{-11}$
$\rightarrow NO^+ + HfONO$	0.15	
$HfO_2^+ + NO \rightarrow NO^+ + HfO_2^+$	1	$\leq 4.6 \times 10^{-11}$
$TaO^+ + 2\,NO \rightarrow TaO_2^+ + N_2O$	1	$\leq 1.5 \times 10^{-11}$
$TaO_2^+ + NO \rightarrow NO^+ + TaO_2$	1	$\leq 1.2 \times 10^{-10}$
$WO^+ + 2\,NO \rightarrow WO_2^+ + N_2O$	1	$\leq 1.2 \times 10^{-11}$
$WO_2^+ + NO \rightarrow NO^+ + WO_2$	0.9	$\leq 4.0 \times 10^{-11}$
$WO_2^+ + 2\,NO \rightarrow WO_3^+ + N_2O$	0.1	
$WO_3^+ + NO \rightarrow NO^+ + WO_3$	1	observed
$ReO^+ + 2\,NO \rightarrow ReO_2^+ + N_2O$	0.5	$\leq 5.4 \times 10^{-11}$
$\rightarrow NO^+ + ReONO$	0.5	
$ReO_2^+ + 2\,NO \rightarrow ReO_3^+ + N_2O$	1	observed
$ReO_3^+ + 2\,NO \rightarrow ReO_4^+ + N_2O$	1	observed
$OsO^+ + 2\,NO \rightarrow OsO_2^+ + N_2O$	0.6	$\leq 4.1 \times 10-11$
$\rightarrow NO^+ + OsONO$	0.3	
$\rightarrow OsO^+(NO) + NO$	0.1	
$OsO_2^+ + NO \rightarrow NO^+ + OsO_2$	1	observed
$OsO^+(NO) + NO \rightarrow OsO^+(NO)_2$	1	observed
$OsO^+(NO)_2 + NO \rightarrow OsO^+(NO)_3$	1	observed
$IrO^+ + NO \rightarrow NO^+ + IrO$	0.95	$\leq 2.4 \times 10^{-10}$
$\rightarrow IrO^+(NO)$	0.05	
$Ir^+(NO) + NO \rightarrow Ir^+(NO)_2$	1	observed
$Pt^+(NO) + NO \rightarrow Pt^+(NO)_2$	1	$\leq 2.9 \times 10^{-11}$
$Pt^+(NO)_2 + NO \rightarrow Pt^+(NO)_3$	1	observed

[a] Product distribution with an accuracy estimated to be 20% for the individual branching fractions. [b] Effective bimolecular rate coefficient first order in NO. The estimated uncertainty is ±30%.

completely rule out some XO_2^+ formation resulting from $(XO^+)^*$ for X = V, Ru, Ta, and Os for which the exothermicity of XO^+ formation exceeds the endothermicity for XO_2^+ formation from reaction 11.

Still higher order oxides were observed with tungsten, WO_3^+, and rhenium, ReO_3^+ and ReO_4^+. Presumably, these are also formed by the thermodynamically-favored termolecular reactions second order in NO.

A number of the oxide cations demonstrated an affinity for NO under the experimental operating conditions employed here. NO ligation was observed in the formation of $CaO^+(NO)$, $ScO^+(NO)$, $TiO^+(NO)$, $VO^+(NO)_{1-3}$, $VO_2^+(NO)_{1-3}$, $SrO^+(NO)$, $SrO_2^+(NO)_{1,2}$, $RuO^+(NO)_{1-3}$, $RuO_2^+(NO)_{1,2}$, $OsO^+(NO)_{1-3}$, and $IrO^+(NO)$. These ligations are expected to take place by termolecular addition in which either He or NO acts as the stabilizing third body.

Also, three atomic cations exhibit an affinity for two NO molecules in the formation of $Rh^+(NO)_2$, $Ir^+(NO)_2$, and $Pt^+(NO)_2$. Again, these ions are expected to be formed by termolecular addition of NO to the XNO^+ nitrosyl cation in which either He or NO acts as the stabilizing third body.

Conclusions

The substantial kinetic results obtained in this study clearly demonstrate that atomic cations initiate a very rich chemistry in their reactions with nitric oxide in the gas phase at room temperature. We have shown that this chemistry can proceed via bimolecular reactions first order in NO and termolecular reactions second order in NO. NO can donate an electron, donate an O-atom in the sequential formation of metal−oxide cations, or simply act as a ligand for some atomic cations and many metal−oxide cations. In some of the ion chemistry NO accepts N atoms leading to the conversion of NO to N_2O or accepts a metal atom leading to the production of metal−nitrosyl molecules. Also, insight is provided into the dependence of the chemistry on the electronic structure of the atomic cation and into the periodic variation in reactivity across and down the periodic table.

Our measurements indicate that the occurrence of bimolecular electron transfer and O-atom transfer from NO to atomic cations is thermodynamically controlled and that NO is not a good N atom donor.

These experiments have demonstrated remarkable termolecular ion chemistry with atomic cations, as well as their oxides, that is second order in NO. We suppose that such chemistry is favorable with NO because of its radical nature that facilitates bond formation, leading to nitrous oxide and metal−nitrosyl molecules. The second-order chemistry with atomic cations is analogous to that which we have reported recently for the diradical oxygen molecule in which a termolecular reaction of Os^+ second order in oxygen was observed to produce O_2^+ and osmium dioxide along with OsO^+ and ozone.[46]

The results with the isolated atomic ions provide *intrinsic* reactivities that may serve as a benchmark for the reactivities of ligated atomic cations toward NO. Our gas-phase measurements also point toward the possibility that metal ions ligated to biological molecules can react in a second-order fashion with NO, perhaps in "pockets" of enhanced NO concentrations that may be present locally in the vicinity of ligated metal ions in biological systems. Such chemistry could produce N_2O and metal nitrosyl molecules in vivo. Analogies also can be drawn with atomic metal ion chemistry occurring on metal surfaces.

Acknowledgment. Continued financial support from the Natural Sciences and Engineering Research Council of Canada is greatly appreciated. Also, we acknowledge support from the National Research Council, the Natural Science and Engineering Research Council and MDS SCIEX in the form of a Research Partnership grant. As holder of a Canada Research Chair in Physical Chemistry, D.K.B. thanks the Canada Research Chair Program for its contributions to this research. We also thank Alfred Khait for his contributions to the literature search and data analysis.

References and Notes

(1) *Nitric Oxide in the Nervous System*; Vincent, Steven R., Ed.; Academic Press: New York, 1995.

(2) Koshland, D. E. *Science* **1992**, *258*, 1861.

(3) Feldman, P. L.; Griffith, O. W.; Stuehr, D. J. *Chem. Eng. News* **1993**, *71* (51), 26.

(4) Richter-Addo, G. B.; Legzdins, P.; Burstyn, J. *Chem. Rev.* **2002**, *102*, 857. This entire issue deals with the chemistry of nitric oxide.

(5) Cadel, R. D. *Particles in the Atmosphere and Space*; Reinhold: New York, **1966**.

(6) Pârvulescu, V. I.; Grange, P.; Delmon, B. *Catal. Today* **1998**, *46*, 233.

(7) Dede_ek, J.; Bortnovsky, O.; Vondrová, A.; Wichterlová, B. *J. Catal.* **2001**, *200*, 160.

(8) Kappas, M. M.; Staley, R. H. *J. Am. Chem. Soc.* **1981**, *103*, 1286.

(9) Blagojevic, V.; Jarvis, M. J. Y.; Flaim, E.; Koyanagi, G. K.; Lavrov, V. V.; Bohme, D. K.*Angew. Chem., Int. Ed.* **2003**, *42*, 4923.

(10) See, for example: (a) Wasser, I. M.; de Vries, S.; Moënne-Loccoz, P.; Schröder, I.; Karlin, K. D. *Chem. Rev.* **2002**, *102*, 1201. (b) Chen, O.; Groh, S.; Liechty, A.; Ridge, D. P. *J. Am. Chem. Soc.* **1999**, *121*, 11910.

(11) Lias, S. G.; Bartmess, J. E.; Liebman, J. F.; Holmes, J. L.; Levin, R. D.; Mallard, W. G. *J. Phys. Chem. Ref. Data* **1988**, *17*: Suppl 1.

(12) Ikezoe, Y.; Matsuoka, S.; Takebe, M.; Viggiano, A. *Gas-Phase Ion−Molecule Reaction Rate Constants Through 1986*; Maruzen Co. Ltd.: Tokyo, 1987.

(13) Adams, N. G.; Smith, D.; Paulson, J. F. *J. Chem. Phys.* **1980**, *72*, 288.

(14) Hamdan,, M.; Copp, N. W.; Birjenshaw, K.; Jones, J. D. C.; Twiddy, N. D. *Int. J. Mass Spectrom. Ion Processes* **1986**, *69*, 191.

(15) Johnson, R.; Castell, F. R.; Biondi, M. A. *J. Chem. Phys.* **1974**, *61*, 5404.

(16) Dheandhanoo, S.; Chatterjee, B. K.; Johnson, R. *J. Chem. Phys.* **1985**, *83*, 3327.

(17) Kappas, M. M.; Staley, R. H. *J. Phys. Chem.* **1981**, *85*, 942.

(18) (a) Koyanagi, G. K.; Lavrov, V.; Baranov, V. I.; Bandura, D.; Tanner, S. D.; McLaren, J. W.; Bohme, D. K. *Int. J. Mass Spectrom.* **2000**, *194*, L1. (b) Koyanagi, G. K.; Baranov, V. I.; Tanner, S. D.; Bohme, D. K. *J. Anal. At. Spectrom.* **2000**, *15*, 1207.

(19) (a) Mackay, G. I.; Vlachos, G. D.; Bohme, D. K.; Schiff, H. I. *Int. J. Mass Spectrom. Ion Phys.* **1980**, *36*, 259. (b) Raksit, A. B.; Bohme, D. K. *Int. J. Mass Spectrom. Ion Processes* **1983/84**, *55*, 69.

(20) Moore, C. E. "Atomic energy levels as derived from the analyses of optical spectra", U.S. National Bureau of Standards, Washington, 1971.

(21) Van Kleef, Th. A. M.; Metsch, B. C. *Physica* **1978**, *C 95*, 251.

(22) Lavrov, V. V.; Blagojevic, V.; Koyanagi, G. K.; Bohme, D. K. *J. Phys. Chem. A* **2004**, *108*, 5610.

(23) (a) Condon, E. U.; Shortley G. H. *The theory of atomic spectra*; Cambridge University Press: 1963; pp 236−237. (b) Garstang R. H. *Monatsch. Not. R. Astron. Soc.* **1962**, *124*, 321.

(24) Petrie, S. Private communication. The adiabatic IE(AsO) has been determined to be 8.290 eV at the CCSD(T)/AUG-cc-pV5Z//CCSD/AUG-cc-pVTZ level of theory, with ZPE calculated at B3-LYP/AUG-cc-pVTZ, with correlation of electrons other than O 1s and As 1s through 3p.

(25) Shul, J. R.; Upschultz, B. L.; Passarella, R.; Keesee, R. G.; Castleman, A. W. *J. Phys. Chem.* **1987**, *91*, 2556.

(26) (a) Su, T.; Chesnavich, W. J. *J. Chem. Phys.* **1982**, *76*, 5183. (b) *Handbook of Chemistry and Physics*, 78th ed.; CRC Press: Boca Raton, FL, 1997.

(27) Jarvis, M. J. Y.; Blagojevic, V.; Koyanagi, G. K.; Bohme, D. K. *Chem. Phys. Lett.* **2005**, *416*, 268.

(28) Schröder, D.; Schwarz, H.; Shaik, S. *Structure and Bonding*; Springer-Verlag: Berlin, Heidelberg, 2000; Vol. 97, pp 91−122.

(29) Freiser, B. S., Ed. *Organnometallic Ion Chemistry*; Kluwer: Dordrecht, 1996.

(30) Sievers, M. R.; Chen, Y.-M.; Armentrout, P. B. *J. Chem. Phys.* **1996**, *105*, 6322.

(31) Chen, Y.-M.; Armentrout, P.B. *J. Chem. Phys.* **1995**, *103*, 618.

(32) Clemmer, D. E.; Dalleska, N. F.; Armentrout, P. B. *Chem. Phys. Lett.* **1992**, *190*, 259.

(33) Blagojevic, V.; Lavrov, V. V.; Orlova, G.; Bohme, D. K. *Chem. Phys. Lett.* **2004**, *389*, 303.

(34) Beyer, M. Dissertation, Technical University München, 1996.

(35) Irikura, K. K.; Beauchamp, J. L. *J. Am. Chem. Soc.* **1989**, *111*, 75.

(36) Pavlov, M.; Blomberg, M. R. A.; Siegbahn, P. E. M.; Wesendrup, R.; Heinemann, C.; Schwarz, H. *J. Phys. Chem. A* **1997**, *101*, 1567.

(37) Zhang, X.-G.; Armentrout, P. B. *J. Phys. Chem. A* **2003**, *107*, 8904.

(38) S. Petrie, private communications. These values were calculated using the QCISD(T)/6-311+G(3df) method; the value for $OA(Se^+)$ does not include a spin−orbit correction.

(39) Blanchet, C.; Duarte, H. A.; Salahub, D. R. *J. Chem. Phys.* **1997**, *106*, 8778.

(40) Zhang L.; Zhou, M. *Chem. Phys.* **2000**, *256*, 185.

(41) Oriedo, J. V.; Russell, D. H. *J. Am. Chem. Soc.* **1993**, *115*, 8376.

(42) Sülzle, D.; Schwarz, H.; Moock, K. H.; Terlouw, J. K. *Int. J. Mass Spectrom. Ion Processes* **1991**, *108*, 269.

(43) Koszinowski, K. Schröder, D.; Schwarz, H.; Holthausen, M. C.; Sauer, J.; Koizumi, H.; Armentrout, P. B. *Inorg. Chem.* **2002**, *41*, 5882.

(44) Khan, F. A.; Steele, D. L.; Armentrout, P. B. *J. Phys. Chem.* **1995**, *99*, 7819.

(45) (a) Rodgers, M. T.; Walker, B.; Armentrout, P. B. *Int. J. Mass Spectrom.* **1999**, *182/83*, 99. (b) Clemmer, D. E.; Dalleska, N. F.; Armentrout, P. B. *J. Chem. Phys.* **1991**, *95*, 7263.

(46) Koyanagi, G. K.; Caraiman, D.; Blagojevic, V.; Bohme, D. K. *J. Phys. Chem. A* **2002**, *106*, 4581.